14. Stage VI *Xenopus* oocytes were obtained by collagenase treatment of ovarian tissue and kept overnight in OR2 medium {82.5 mM NaCl, 2.5 mM KCl, 1 mM $CaCl_2$, 1 mM $MgCl_2$, 1 mM Na_2HPO_4, 5 mM Hepes (pH 7.8) [R. A. Wallace, D. W. Jared, J. N. Dumont, M. W. Sega, *J. Exp. Zool.* **184**, 321 (1973)]}. Oocytes were treated with progesterone or microinjected with purified recombinant malE-Mos, incubated for 8 to 10 hours, and then collected individually and frozen on dry ice. Individual oocytes were lysed by the addition of ice cold lysis buffer (50 to 100 μl) [100 mM NaCl, 50 mM β-glycerolphosphate (pH 7.4), 10 mM EDTA, 2 mM NaF, 1 mM sodium orthovanadate, leupeptin (10 μg/ml), chymostatin (10 μg/ml), and pepstatin (10 μg/ml)], and crude cytoplasm was collected after centrifugation for 2 min in a Beckman E microcentrifuge with right angle rotor. Cytoplasm was promptly added to 0.2 volumes of 6× Laemmli sample buffer. Proteins were separated on 10.5% (100:1 acrylamide:bisacrylamide) polyacrylamide SDS gels and transferred to polyvinylidene difluoride membranes. p42 MAP kinase was detected with polyclonal antiserum DC3 [K.-M. Hsiao, S.-y. Chou, S.-J. Shih, J. E. Ferrell Jr., *Proc. Natl. Acad. Sci. U.S.A.* **91**, 5480 (1994)].
15. Assume that the response y (MAPK phosphorylation or activation) of an individual oocyte to a stimulus x (progesterone or malE-Mos concentration) is well approximated by a Hill equation, as is found experimentally for MAPK responses in extracts (*8*):

$$y = \frac{x^{n_H}}{k^{n_H} + x^{n_H}} \quad (1)$$

Assume that individual oocytes have different values of k, which represents the concentration of x at which the oocyte's response is half-maximal, and that the distribution of oocytes among various values of k is given by

$$D = \frac{dN}{dk} \quad (2)$$

where

$$N = \frac{k^m}{a^m + k^m} \quad (3)$$

The exponent m defines the variability of the oocytes; the larger the value of m, the less variability in the concentration of stimulus at which the oocytes respond half-maximally. The constant a represents the stimulus concentration by which half of the oocytes have responded at least half-maximally. The distribution of oocytes among various values of the response y is given by

$$F = -\frac{dN}{dy} \quad (4)$$

To evaluate Eq. 4, we solve for k in terms of x and y using Eq. 1, and then substitute the result into Eq. 3:

$$k = x\left(\frac{1-y}{y}\right)^{1/n_H} \quad (5)$$

$$N = \frac{x^m\left(\frac{1-y}{y}\right)^{m/n_H}}{a^m + x^m\left(\frac{1-y}{y}\right)^{m/n_H}} \quad (6)$$

Taking the derivative of N with respect to y to yields the desired formula:

$$F = \frac{-ma^m x^m\left(\frac{1-y}{y}\right)^{m/n_H}}{n\left[a^m + x^m\left(\frac{1-y}{y}\right)^{m/n_H}\right]^2 (y-1)y} \quad (7)$$

Equation 7 describes how a population of oocytes is distributed among various values of the response y for a given level of stimulus x and given values of the steepness of the oocytes' individual responses (n_H) and the tightness of the oocyte-to-oocyte variation (m). This equation was used to calculate the distributions shown in Fig. 1D and to infer values of the Hill coefficient n_H for the experimentally determined oocyte distributions (Figs. 1 and 2).
16. This lower bound is calculated as the smallest Hill coefficient for which the probability that none of the 209 oocytes will have MAPK-P between 10% and 90% is less than 0.05.
17. A. R. Nebreda and T. Hunt, *EMBO J.* **12**, 1979 (1993); J. Posada, N. Yew, N. G. Ahn, G. F. Vande Woude, J. A. Cooper, *Mol. Cell. Biol.* **13**, 2546 (1993); E. K. Shibuya and J. V. Ruderman, *Mol. Biol. Cell* **4**, 781 (1993).
18. W. T. Matten, T. D. Copeland, N. G. Ahn, G. F. Vande Woude, *Dev. Biol.* **179**, 485 (1996); L. M. Roy *et al.*, *Oncogene* **12**, 2203 (1996).
19. M. Nishizawa *et al.*, *EMBO J.* **12**, 4021 (1993).
20. Evidence that Mos accumulation depends on Cdc2 function can be found in A. R. Nebreda, J. V. Gannon, T. Hunt, *ibid.* **14**, 5597 (1995).
21. Here we shall derive an expression for the steady-state phosphorylation and activity of MAPK in response to malE-Mos for the system shown schematically in Fig. 3A. If the response of MAPK to Mos is well approximated by a Hill function with a Hill coefficient of n_H for MAPK activation and n_H' for MAPK phosphorylation, as it is in extracts (*8*), then the steady-state level of active MAPK is

$$\text{active MAPK}_{ss} = \text{MAPK}_{tot}\frac{(\text{Mos-P}_{ss} + \text{malE-Mos})^{n_H}}{\text{EC}_{50}^{n_H} + (\text{Mos-P}_{ss} + \text{malE-Mos})^{n_H}} \quad (8)$$

and the steady-state level of phosphorylated MAPK is

$$\text{phos. MAPK}_{ss} = \text{MAPK}_{tot}\frac{(\text{Mos-P}_{ss} + \text{malE-Mos})^{n_H'}}{\text{EC}_{50}'^{n_H'} + (\text{Mos-P}_{ss} + \text{malE-Mos})^{n_H'}} \quad (9)$$

where EC_{50} is the median effective concentration. The rate of Mos phosphorylation is k_2 [$MAPK_{active}$][Mos] (where the square brackets indicate concentration), and so the steady-state concentration of Mos-P is

$$\text{Mos-P}_{ss} = \frac{k_1k_2}{k_{-1}k_{-2}}[\text{MAPK}_{active}] \quad (10)$$

Substituting Eq. 8 into Eq. 10 yields

$$\text{Mos-P}_{ss} - \left\{\frac{k_1k_2}{k_{-1}k_{-2}}[\text{MAPK}_{tot}] \times \frac{(\text{Mos-P}_{ss} + \text{malE-Mos})^{n_H}}{\text{EC}_{50}^{n_H} + (\text{Mos-P}_{ss} + \text{malE-Mos})^{n_H}}\right\} = 0 \quad (11)$$

The roots of this equation are the possible steady-state concentrations of Mos-P. This equation was solved numerically with Mathematica 2.2.2 (Wolfram Research, Champaign, IL). Equations 8 and 9 were then used to calculate the corresponding concentrations of active and phosphorylated MAPK (Fig. 3B). Other things being equal, as the Hill coefficient increases, the concentration of malE-Mos needed for the switching between an off state and an on state becomes larger and the "completeness" of the switching becomes greater. A Hill coefficient of 3 for MAPK phosphorylation and of 5 for MAPK activation is sufficient to produce switching with a threshold and completeness that agree well with what is observed experimentally (Fig. 3B).
22. The response of MAPK phosphorylation to malE-Mos, as measured here, is expected to exhibit a Hill coefficient of at least half that seen for the response of MAPK activation to malE-Mos, measured previously (*8*).
23. Bistability in other systems is discussed in B. Novak and J. J. Tyson, *J. Cell Sci.* **106**, 1153 (1993); C. D. Thron, *Biophys. Chem.* **57**, 239 (1996); J. J. Tyson, B. Novak, G. M. Odell, K. Chen, C. D. Thron, *Trends Biochem. Sci.* **21**, 89 (1996); and B. N. Kholodenko, J. B. Hoek, H. V. Westerhoff, G. C. Brown, *FEBS Lett.* **414**, 430 (1997).
24. P. B. Chock, S. G. Rhee, E. R. Stadtman, *Annu. Rev. Biochem.* **49**, 813 (1980).
25. We thank M. Murakami and G. Vande Woude for providing malE-Mos plasmids and C.-Y. F. Huang for expressing and purifying malE-Mos. Supported by a grant from NIH (GM46383) and the Stanford University Cancer Biology Training Grant (CA09302).

3 November 1997; accepted 25 March 1998

Role of Rac1 and Oxygen Radicals in Collagenase-1 Expression Induced by Cell Shape Change

Farrah Kheradmand, Erica Werner, Patrice Tremble,* Marc Symons, Zena Werb†

Integrin-mediated reorganization of cell shape leads to an altered cellular phenotype. Disruption of the actin cytoskeleton, initiated by binding of soluble antibody to α5β1 integrin, led to increased expression of the collagenase-1 gene in rabbit synovial fibroblasts. Activation of the guanosine triphosphate–binding protein Rac1, which was downstream of the integrin, was necessary for this process, and expression of activated Rac1 was sufficient to increase expression of collagenase-1. Rac1 activation generated reactive oxygen species that were essential for nuclear factor kappa B–dependent transcriptional regulation of interleukin-1α, which, in an autocrine manner, induced collagenase-1 gene expression. Remodeling of the extracellular matrix and consequent alterations of integrin-mediated adhesion and cytoarchitecture are central to development, wound healing, inflammation, and malignant disease. The resulting activation of Rac1 may lead to altered gene regulation and alterations in cellular morphogenesis, migration, and invasion.

Modifications of cell shape are crucial for tissue morphogenesis, cell migration, and invasion. These alterations in cell morphology are thought to rely on the organization of the actin cytoskeleton and the modulation of cell adhesion. Changes in cell morphology lead to specific signaling from cell adhesion receptors and a consequent change of gene expression (*1*), including genes encoding the matrix metalloprotein-

ase (MMP) family, which includes collagenase-1 (CL-1) and stromelysin-1 (*2*, *3*). The organization and dynamics of the various structures that constitute the actin cytoskeleton are controlled by members of the Rho family of small guanosine triphosphate (GTP)–binding proteins (*4*). Lysophosphatidic acid–induced formation of stress fiber is governed by Rho, growth factor–stimulated extension of lamellipodia and ruffling are regulated by Rac, and filopodia formation is controlled by Cdc42. We have studied the signal transduction cascade initiated by alteration of integrin-controlled adhesion that leads to increased expression of the gene encoding CL-1 in rabbit synovial fibroblasts (RSFs).

Expression of CL-1 is increased when RSFs adhere and spread on specific integrin ligands or when the cells round and disrupt the actin cytoskeleton (*5*). These processes probably involve two distinct pathways, because they differ in integrin specificity and kinetics. Ligation of α5β1 integrin with an adhesion-perturbing monoclonal antibody (mAb) to α5β1 in solution (*5*) reduced the organized actin microfilament cytoskeleton and induced CL-1 expression in RSFs (Fig. 1A). We tested whether Rho family guanosine triphosphatases (GTPases) transduce the signals from integrin ligation that lead to *CL-1* expression by transfecting RSFs with constructs encoding the dominant interfering mutants Rac1N17, RhoAN19, and Cdc42N17 (*6*–*8*). Increased expression of CL-1 caused by addition of soluble mAb to α5, which inhibits substrate adhesion of cells and causes cell rounding, was abrogated by transient expression of Rac1N17 but not by expression of RhoAN19 or Cdc42N17 (Fig. 1B). In contrast, enhanced expression of CL-1 caused by spreading of the cells via α5β1 on the same mAb bound to the culture dishes as a substrate was independent of Rac1 (Fig. 1B). These data indicate that α5 integrin–mediated spreading and rounding have distinct signaling pathways. Treatment of cells with cytochalasin D (CD) rounds cells directly by disrupting the actin-dependent cytoarchitecture and increases expres-

F. Kheradmand, Department of Medicine, University of California, San Francisco, CA, USA.
E. Werner, P. Tremble, Z. Werb, Department of Anatomy, University of California, San Francisco, CA 94143-0750, USA.
M. Symons, Onyx Pharmaceuticals, Richmond, CA 94806, USA.
*Present address: Baxter Healthcare Corp., Round Lake, IL 60073, USA.
†To whom correspondence should be addressed. E-mail: zena@itsa.ucsf.edu

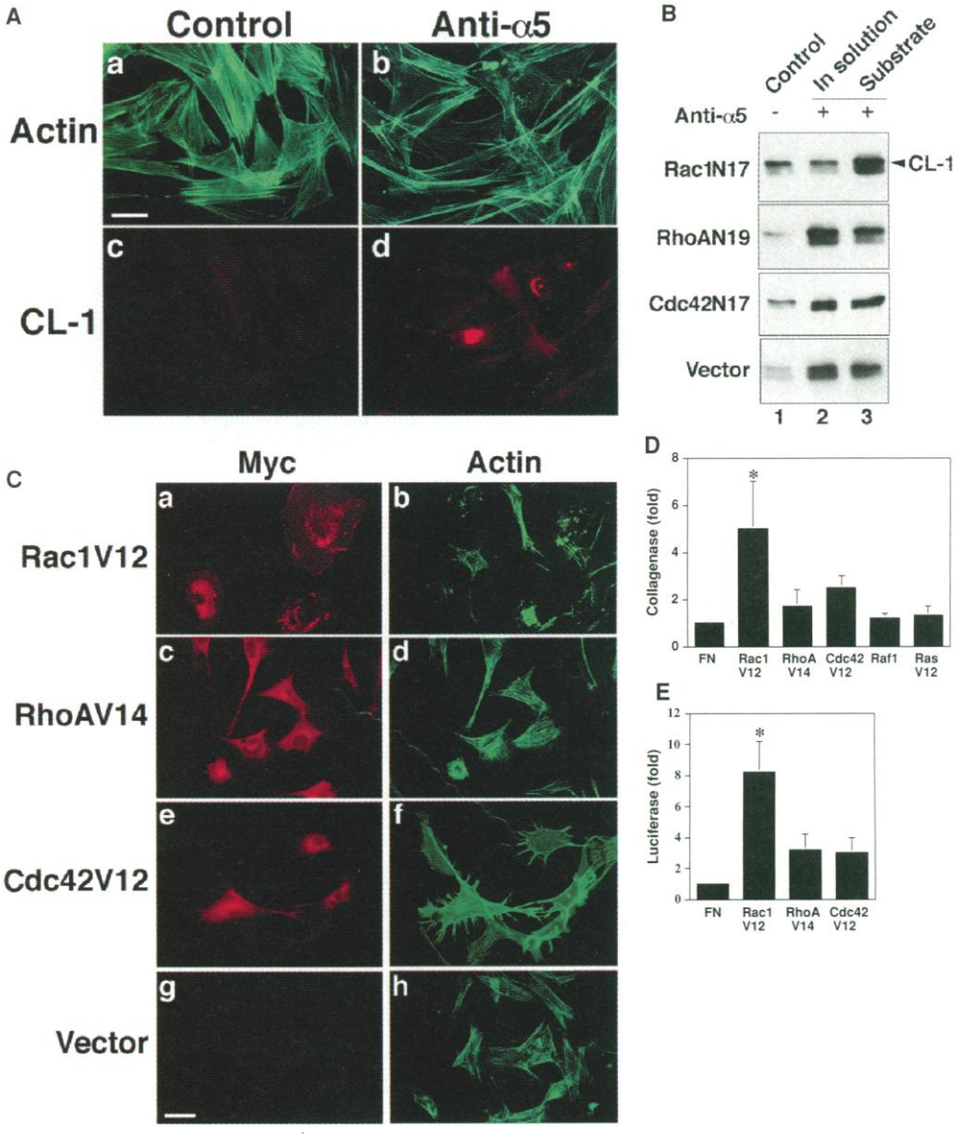

Fig. 1. Effect of actin reorganization and Rho GTPase on CL-1 expression. (**A**) Actin reorganization and expression of CL-1. RSFs were cultured on fibronectin (FN) substrates (*3*, *10*) in serum-free medium for 18 hours in the absence (a and c) or presence (b and d) of function-perturbing BIIG2 anti-α5 (4 μg/ml). The cultures were stained simultaneously for fibrillar actin with fluorescein-phalloidin (a and b) and CL-1 with biotinylated mAb to CL-1 (c and d) followed by Texas Red–labeled streptavidin (*3*). (**B**) Requirement of Rac1 for cell shape–dependent expression of CL-1. RSFs transiently expressing β-Gal (control) or dominant interfering mutants RacN17, RhoN19, or CdcN17 (*6*, *8*) were cultured on FN with anti-α5 in solution (4 μg/ml) or on immobilized anti-α5 (*3*, *8*). CL-1 was detected by immunoblotting of medium (30 μl) after incubation for 18 hours with 1.5×10^4 transfected cells (*5*). (**C**) Reorganization of actin in RSFs expressing activated Rho GTPases. RSF were stained with mAb to Myc and with Texas Red–labeled antibody to mouse IgG to detect the Myc epitope tag of the transfected GTPases (*6*, *7*) (a, c, e, and g) or with fluorescein-phalloidin for actin (b, d, f, and h). (**D**) Analysis by slot immunoblot (*3*) of CL-1 in medium conditioned for 24 hours by RSFs transiently transfected with members of the Ras superfamily. Data are expressed as fold induction relative to control (FN) and are the mean ± SEM of three separate experiments. (**E**) Transcriptional regulation of CL-1 by Rac1. RSFs were transfected with activated GTPases and the hCL-1/Luc construct. The transfected RSFs were plated onto wells coated with FN for 18 hours, and the luciferase reporter activity was determined (*12*). Data are expressed as fold induction compared with induction of control β-Gal–transfected cells (FN) and are the mean ± SEM of the results of six experiments. (**D** and **E**) Values showing statistical significance in comparison with controls ($P < 0.05$, analysis of variance) are indicated by an asterisk. Scale bar in (A) and (C), 20 μm.

sion of CL-1 (*2*). This effect of CD was not inhibited by expression of Rac1N17 (*9*), indicating that Rac1 either acts upstream of shape changes in the signaling pathway or does not participate in the effect of CD. Rac1N17 alone did not alter expression of CL-1. Expression of a dominant negative mitogen-activated protein (MAP) kinase kinase (MEK) construct (*6*), which interferes with activation of the MAP kinase pathway, had no effect on basal expression of CL-1 or on CL-1 expression induced by antibody to α5 (anti-α5) in solution (*9*).

If Rac1 contributes to increased expression of CL-1 in response to binding of soluble anti-α5, then constitutively activated forms of Rac1 alone should increase expression of CL-1. Transient expression of Rac1V12 reduced stress fibers in >90% of cells, stimulated formation of actin-rich lamellipodia and pinocytosis, and caused the formation of some multinucleated cells (Fig. 1C). In contrast, RhoAV14 increased formation of stress fiber in >90% of cells. Cells expressing Cdc42V12 had many filopodia and complete dissolution of stress fibers. At equivalent amounts of expression, Rac1V12 was effective in increasing CL-1 expression, whereas RhoAV14 and Cdc42V12 had little effect (Fig. 1D). Oncogenic RasV12 (*6*) or Raf-1 (*10*) did not increase expression of CL-1 (Fig. 1E).

We used a promoter-luciferase construct containing the −517- to +63-bp segment of the human collagenase promoter (hCL-1/Luc), which includes an AP1 site, a PEA3 site, a transforming growth factor–β (TGF-β) inhibitory element (TIE), and two AP2 sites (*11*, *12*) to determine whether these GTPases altered transcription of the gene encoding CL-1. Transfection of Rac1V12 with the hCL-1/Luc construct increased ex-

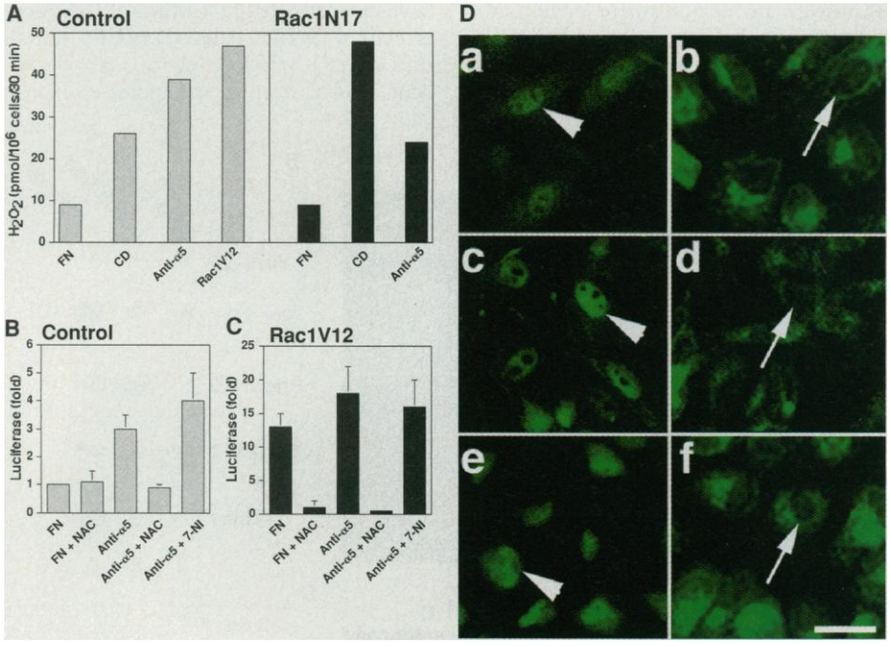

Fig. 2. Actin reorganization–dependent induction of hCL-1/Luc expression mediated by production of ROS. (**A**) ROS production by RSFs. Control cells transiently expressing Rac1N17 or Rac1V12 were plated on FN in the presence of soluble anti-α5 or CD as indicated and assessed for H_2O_2 production (*21*). (**B** and **C**) CL-1 promoter transcription, measured as luciferase expression, was induced by soluble anti-α5 in (B) control cells or (C) cells transiently expressing Rac1V12 treated as indicated with 50 mM NAC or 7-nitroindazole (7-NI). Data are expressed as fold induction in comparison with control cells plated on FN alone and are the mean ± SEM of four experiments. (**D**) Cell shape–dependent translocation of NF-κB into nuclei of RSFs (*22*) and inhibition by NAC. Rac1V12-transfected (a) or control RSFs (b through f) were plated on cover slips coated with FN (a through e) or immobilized anti-α5 (f) for 3 hours and then treated with 50 μM H_2O_2 for 3 hours (c) or incubated with 50 mM NAC (for 1 hour) (d) before treatment with 50 μM H_2O_2 for 3 hours, or treated with anti-α5 (4 μg/ml) in solution for 3 hours (e) or left untreated for 3 hours (a and b). Arrows, cytoplasmic NF-κB (p65); arrowheads, nuclear NF-κB (p65). Scale bar, 20 μm.

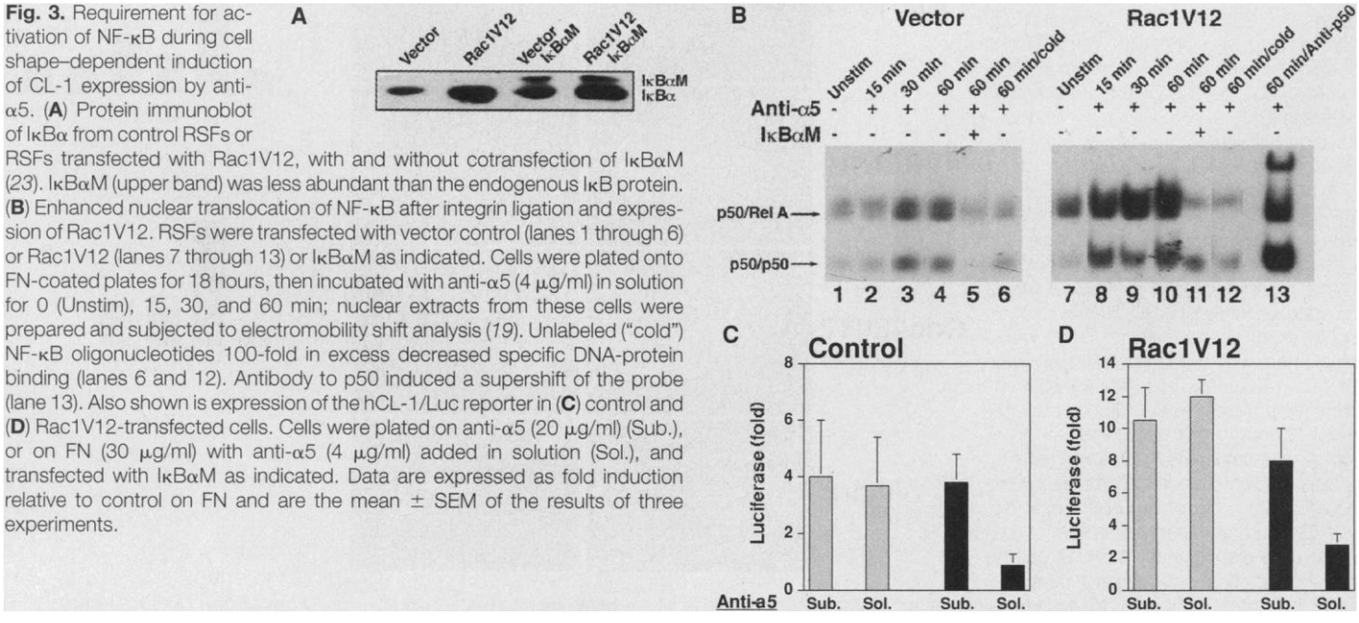

Fig. 3. Requirement for activation of NF-κB during cell shape–dependent induction of CL-1 expression by anti-α5. (**A**) Protein immunoblot of IκBα from control RSFs or RSFs transfected with Rac1V12, with and without cotransfection of IκBαM (*23*). IκBαM (upper band) was less abundant than the endogenous IκB protein. (**B**) Enhanced nuclear translocation of NF-κB after integrin ligation and expression of Rac1V12. RSFs were transfected with vector control (lanes 1 through 6) or Rac1V12 (lanes 7 through 13) or IκBαM as indicated. Cells were plated onto FN-coated plates for 18 hours, then incubated with anti-α5 (4 μg/ml) in solution for 0 (Unstim), 15, 30, and 60 min; nuclear extracts from these cells were prepared and subjected to electromobility shift analysis (*19*). Unlabeled ("cold") NF-κB oligonucleotides 100-fold in excess decreased specific DNA-protein binding (lanes 6 and 12). Antibody to p50 induced a supershift of the probe (lane 13). Also shown is expression of the hCL-1/Luc reporter in (**C**) control and (**D**) Rac1V12-transfected cells. Cells were plated on anti-α5 (20 μg/ml) (Sub.), or on FN (30 μg/ml) with anti-α5 (4 μg/ml) added in solution (Sol.), and transfected with IκBαM as indicated. Data are expressed as fold induction relative to control on FN and are the mean ± SEM of the results of three experiments.

pression of the luciferase reporter, similar to what was observed for endogenous CL-1 production, whereas expression of RhoAV14 or Cdc42V12 did not increase expression of luciferase significantly (f in Fig 1C). In cells transfected with Rac1N17, CD increased expression of luciferase 21-fold (9).

In phagocytic cells, Rac constitutes part of the multimolecular β-nicotinamide adenine dinucleotide phosphate (NADH)–oxidase complex that generates the reactive oxygen species (ROS) superoxide free radical (O_2^-) and its dismutation product H_2O_2 (13). The enzymes that generate ROS in fibroblasts have not been identified. However, RSFs treated with anti-α5 in solution or with CD, or transfected with Rac1V12, produced H_2O_2 (Fig. 2A). CD, but not anti-α5, effectively induced H_2O_2 production in cells transfected with Rac1N17 (Fig. 2A). Scavengers of oxygen free radicals *N*-acetyl-L-cysteine (NAC) or Tiron (1,2-dihydroxybenzene-3,5-disulfonate) abrogated anti-α5– and Rac1V12-mediated expression of the hCL-1/Luc reporter, whereas inhibition of reactive nitrogen species by 7-nitroindazole (Fig. 2, B and C) and N^G-nitro-L-arginine methyl ester (9) had no effect. NAC also inhibited secretion of CL-1 induced by soluble anti-α5 and CD (9).

The nuclear factor kappa B (NF-κB)/Rel family of transcription factors, which are activated by stimulants such as H_2O_2 (14), mediated Rac1-induced expression of CL-1. Cytoplasmic NF-κB exists in an inactive complex consisting of DNA-binding components (p50/RelA) bound to an inhibitory component of the IκBα family (14). Treatment of RSFs with anti-α5 in solution or with 50 μM H_2O_2, but not with immobilized anti-α5, induced rapid nuclear translocation of NF-κB that was blocked by incubation of the cells with 50 mM NAC (Fig. 2C), which is consistent with a role for NF-κB downstream of ROS in regulating expression of CL-1. Cells expressing Rac1V12 that constitutively expressed CL-1 also showed a nuclear localization of NF-κB (Fig. 2C). Expression of IκBαM, a transdominant-negative mutant of IκBα (15), inhibited activation and translocation of NF-κB into the nucleus (16) (Fig. 3, A and B) and repressed expression of both endogenous CL-1 (9) and hCL-1/Luc (Fig. 3, C and D) in cells treated with soluble anti-α5 or transfected with Rac1V12. Nuclear extracts prepared from Rac1V12 transfectants showed constitutive activation of NF-κB, which was increased by soluble anti-α5 (Fig. 3B).

Although NF-κB can transactivate genes directly, the hCL-1/Luc construct has no NF-κB/Rel consensus sequence, indicating that NF-κB-mediated induction of CL-1 expression is indirect. Because interleukin-1 (IL-1), which is an NF-κB–regulated protein, can act in an autocrine manner to induce CL-1 in primary fibroblasts (17), we investigated the role of IL-1α in integrin-mediated expression of CL-1. Treatment of RSFs with anti-α5 in solution stimulated synthesis of IL-1α mRNA (9), secretion of the protein (Fig. 4, A and B), and expression of the hCL-1/Luc reporter (Fig. 3, C and D). Expression of Rac1V12 caused a 28-fold increase in IL-1 secretion, which was increased further by treatment with soluble anti-α5. The ROS inhibitor NAC blocked the IL-1 expression induced by soluble anti-α5 and Rac1V12 (Fig. 4, A and B). These data indicate that increased expression of the IL-1 gene is a consequence of integrin- and Rac1-mediated alteration of cell shape and of ROS generated in this pathway. IL-1 expression was required for shape-dependent expression of CL-1. IL-1 receptor antagonist (IL-1RA), a competitive inhibitor for IL-1 interaction with its receptor, suppressed CL-1 expression induced by anti-α5 in solution, Rac1V12 (Fig. 4C), or CD (9, 17). These data indicate that an IL-1–controlled autocrine loop mediates the induction of CL-1 caused by changes in cell shape.

Our results indicate that the Rac GTPase is an essential component in the signaling cascade initiated by integrin-mediated cell rounding that leads to the expression of CL-1. MMPs are crucial in cell migration and tumor invasion (18, 19). Rac1 has been implicated in invasion of lymphoma and epithelial cells and is essential for growth factor–induced migration of fibroblasts (4, 19). Although Ras is important in some types of integrin signaling (20), and acts upstream of Rac1 in growth factor–mediated directed migration in mammary epithelial cells and Rat1 fibroblasts (19), we showed a distinct signaling pathway through Rac1 that is functional and separate from a Ras-mediated signaling cascade. Interference with α5 integrin–mediated cell adhesion activated Rac1, which then caused generation of ROS, induced activation of NF-κB, and led to induction of IL-1, an autocrine inducer of CL-1 expression. This pathway is distinct from that activated by α5 integrin–dependent spreading, which also leads to expression of CL-1 and requires rapid activation of AP1 (3), but does not require Rho-family GTPases, ROS, NF-κB activation, or IL-1 expression. Thus, exposure of cells to a soluble integrin ligand produces cell rounding, whereas exposure to an insoluble integrin ligand induces spreading. In fibroblasts, these distinct changes in cell shape trigger diverse signaling pathways, which happen to impinge on the gene encoding CL-1. Regulation of MMPs through integrin-mediated disruption of the actin cytoskeleton and alteration of cell form may influence developmental, migratory, and invasive properties of cells. Modifications in the extracellular matrix composition change both integrin-mediated signaling (20) and proteolysis (18) and, through these mechanisms, are strong determinants of cell behavior in normal and pathological settings.

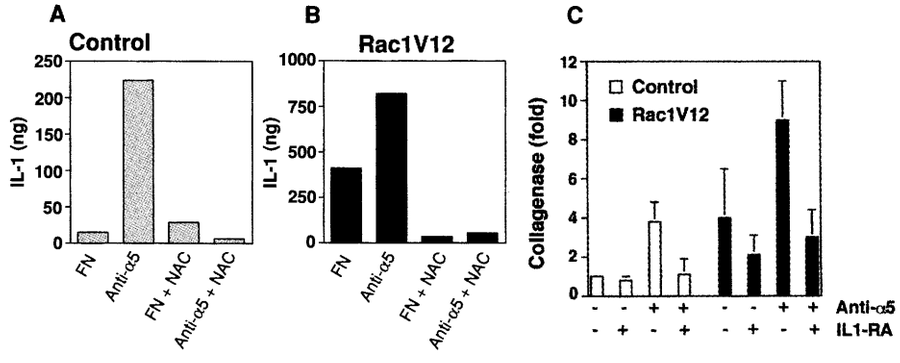

Fig. 4. Cell shape–dependent induction of IL-1 expression and IL-1–dependent CL-1 expression. Expression of IL-1 (24) in (**A**) control and (**B**) Rac1V12-transfected cells. Cells were exposed to anti-α5 or 50 mM NAC as indicated. Data are expressed as means of two separate experiments done in duplicate. (**C**) Control and Rac1V12-transfected cells were plated onto FN-coated wells and were left untreated or were treated with anti-α5 in solution (4 μg/ml) in the presence or absence of IL-1RA (10 ng/ml). Medium from 5 × 10^4 cells cultured for 18 hours was analyzed for CL-1 by immunoblotting (3). Data are expressed as *n*-fold induction in comparison with the amount of CL-1 induced from control cells plated on FN and are shown as the mean ± SEM of three separate experiments.

REFERENCES AND NOTES

1. C. S. Chen, M. Mrksich, S. Huang, G. M. Whitesides, D. E. Ingber, *Science* **276**, 1425 (1997); D. Dash, M. Aepfelbacher, W. Siess, *J. Biol. Chem.* **270**, 17321 (1995); V. M. Weaver *et al.*, *J. Cell Biol.* **137**, 231 (1997); C. D. Roskelley, A. Srebrow, M. J. Bissell, *Curr. Opin. Cell Biol.* **7**, 736 (1995).
2. E. D. Harris Jr., J. J. Reynolds, Z. Werb, *Nature* **257**, 243 (1975); J. Aggeler, S. M. Frisch, Z. Werb, *J. Cell Biol.* **98**, 1662 (1984); P. Tremble, R. Chiquet-Ehrismann, Z. Werb, *Mol. Biol. Cell* **5**, 439 (1994); C. D. Roskelley and M. J. Bissell, *Biochem. Cell Biol.* **73**,

391 (1995); J. J. Tomasek *et al.*, *J. Biol. Chem.* **14**, 7482 (1997).
3. P. Tremble, C. H. Damsky, Z. Werb, *J. Cell Biol.* **129**, 1707 (1995); P. Huhtala *et al.*, *ibid.*, p. 867.
4. A. Ridley, *Curr. Biol.* **6**, 1256 (1996); N. Tapon and A. Hall, *Curr. Opin. Cell Biol.* **9**, 86 (1997); P. T. Hawkins *et al.*, *Curr. Biol.* **5**, 393 (1995).
5. Z. Werb, P. M. Tremble, O. Behrendtsen, E. Crowley, C. H. Damsky, *J. Cell Biol.* **109**, 877 (1989).
6. R. G. Qiu, J. Chen, D. Kirn, F. McCormick, M. Symons, *Nature* **374**, 457 (1995).
7. R. G. Qiu, A. Abo, F. McCormick, M. Symons, *Mol. Cell Biol.* **17**, 3449 (1997); R. G. Qiu, J. Chen, F. McCormick, M. Symons, *Proc. Natl. Acad. Sci. U.S.A.* **92**, 11781 (1995).
8. RSFs (*2*) were cultured in Dulbecco's modified Eagle's medium (DMEM) supplemented with 10% fetal bovine serum (FBS; Hyclone, Denver, CO). RSFs used between passages 4 through 15 were subcultured 24 hours before transfection or other experimental procedures. We used adenovirus-mediated transfection for transient transfection: RSFs (4×10^6) were harvested from subconfluent plates with trypsin (0.05%; Cell Culture Facility, University of California, San Francisco), were mixed at a 1:40 final dilution of a replication-defective mutant of human adenovirus-5 (GPT-Ad5) [J. R. Forsayeth and P. D. Garcia, *Biotechniques* **17**, 354 (1994)] and DEAE-Dextran (80 μg/ml; Pharmacia), and were brought to 5 ml in DMEM. Then 10 μg of each plasmid was added, after which the mixture was plated onto culture dishes and incubated for 2.5 hours in a 5% CO_2-enriched atmosphere at 37°C. At the end of the incubation, cells were rinsed with 2 ml of 10% dimethyl sulfoxide in phosphate-buffered saline (Ca^{2+}- and Mg^{2+}-free) for 2 min to stop transfection and to remove nonadherent cells, and 10 ml of DMEM supplemented with FBS (10%) was added. Cells were incubated overnight to recover. We routinely obtained 70 to 90% efficiency of transfection in RSFs, as determined with cytomegalovirus promoter–driven green fluorescent protein or β-galactosidase (β-gal) expression vector and detection by fluorescence or by in situ staining with 5-bromo-4-chloro-3-indolyl-β-D-galactosidase (X-gal), respectively. Transfected cells were then replated onto 24-well plates coated with fibronectin (FN; 30 μg/ml) or anti-α5 (BIIG2; 20 μg/ml) or onto FN-coated plates with anti-α5 (4 μg/ml) in solution (*3*). Cells were incubated in DMEM supplemented with lactalbumin hydrolysate (0.2%) for 18 hours.
9. F. Kheradmand, E. Werner, P. Tremble, M. Symons, Z. Werb, unpublished data.
10. J. T. Bruder, G. Heidecker, U. R. Rapp, *Genes Dev.* **6**, 545 (1992).
11. P. Angel *et al.*, *Mol. Cell Biol.* **7**, 2256 (1987).
12. The human CL-1 promoter luciferase reporter construct was made by cloning the −517 to +63 nucleotide sequences of the 5′-flanking region of human CL-1 promoter, which contains a minimal promoter from human genomic DNA, by polymerase chain reaction–based cloning. A Hind III deletion site was engineered into the 3′ end of the promoter fragment. This fragment was then subcloned into the Kpn 1–Hind III site in PGL3 plasmid (Promega) to give the (−517 to +63) hCL-1/Luc construct. Transfected cells were lysed in luciferase lysis buffer (Promega), and 3 μg of protein as analyzed by the Bradford method was assayed for luciferase activity with a luminometer. Transfection efficiencies, determined by cotransfection with β-Gal construct (2 μg), were essentially similar.
13. A. Abo, M. R. Webb, A. Grogan, A. W. Segal, *Biochem. J.* **298**, 585 (1994); A. W. Segal and A. Abo, *Trends Biochem. Sci.* **18**, 43 (1993); X. Xu, D. C. Barry, J. Settleman, M. A. Schwartz, G. M. Bokoch, *J. Biol. Chem.* **269**, 23569 (1994).
14. H. M. Lander, *FASEB J.* **11**, 118 (1997); G. Bonizzi *et al.*, *Eur. J. Biochem.* **242**, 544 (1996); S. Miyamoto and I. M. Verma, *Adv. Cancer Res.* **66**, 255 (1995); A. Ray and K. E. Prefontaine, *Proc. Natl. Acad. Sci. U.S.A.* **91**, 752 (1994); A. S. Baldwin Jr., *Annu. Rev. Immunol.* **14**, 649 (1996).
15. D. J. Van Antwerp, S. J. Martin, T. Kafri, D. R. Green, I. M. Verma, *Science* **274**, 787 (1996).
16. Nuclear protein extracts [D. S. Finbloom *et al.*, *Mol. Cell Biol.* **14**, 2113 (1994)] (5 μg) were incubated with a ^{32}P-labeled NF-κB–specific oligonucleotide (Promega) and subjected to electromobility shift analysis as described by the manufacturer.
17. J. A. West-Mays, K. J. Strissel, P. M. Sadow, M. E. Fini, *Proc. Natl. Acad. Sci. U.S.A.* **92**, 6768 (1995).
18. Z. Werb, *Cell* **91**, 439 (1997); L. M. Coussens and Z. Werb, *Chem. Biol.* **3**, 895 (1996).
19. B. Anand-Apte *et al.*, *J. Biol. Chem.* **272**, 30688 (1997); P. J. Keely, J. K. Westwick, I. P. Whitehead, J. D. Channing, L. V. Parise, *Nature* **390**, 632 (1997); F. Michiels, G. G. M. Habets, J. C. Stam, R. van der Kammen, J. G. Collard, *ibid.* **375**, 338 (1995).
20. T. H. Lin *et al.*, *J. Cell Biol.* **136**, 1385 (1997); P. E. Hughes *et al.*, *Cell* **88**, 521 (1997); K. M. Yamada and B. Geiger, *Curr. Opin. Cell. Biol.* **9**, 76 (1997); M. A. Schwartz, M. D. Schaller, M. H. Ginsberg, *Annu. Rev. Cell Dev. Biol.* **11**, 549 (1995).
21. ROS production was detected as a transient increase in catalase (200 U/ml)-sensitive oxidation of homovanillic acid [W. Ruch, P. Cooper, M. Baggiolini, *J. Immunol. Methods* **63**, 347 (1983)]. For each treatment, untransfected or Rac1N17-transfected fibroblasts (1×10^6) were plated on FN in seven replicates, and then stimulated with anti-α5 in solution (4 μg/ml) or with CD (2 μg/ml). In the next 2 hours, one plate was harvested every 20 min. For Rac1V12- and Rac1N17-transfected cells, the H_2O_2 production was measured over 2 hours, starting 24 hours after transfection. The results are the average of the integrated peak detected in at least three independent experiments.
22. RSFs were fixed in 4% paraformaldehyde, permeabilized with Triton-X100, and then stained with a polyclonal antibody to the p65 (Rel) component of NF-κB (Santa Cruz Biotech) and with a fluorescein-conjugated antibody to rabbit Ig.
23. Cell lysates (40 μg) were resolved by SDS–polyacrylamide gel electrophoresis (12% gel) and immunoblotted with polyclonal to IκB antibody (Santa Cruz Biotech). Supershift analysis was done by incubating nuclear extracts (5 μg) with antibody to the p50 component of NF-κB (1 μg; Santa Cruz Biotech) for 30 min at ambient temperature.
24. IL-1α was detected by slot immunoblotting (*3*) of medium (100 μl) after 18 hours of culture with 1.5 $\times 10^4$ with a polyclonal antibody to rabbit IL-1α (Endogen).
25. We thank C. Damsky for the gift of anti-α5 (BIIG2) and critical reading of the manuscript and D. Williams-Herman for assistance in preparing the hCL-1/Luc construct. Supported by NIH grants DE10306 and AR20684 (Z.W.), a fellowship from the American Lung Association, a Mentored Clinician Scientist Award (HL03732) (F.K.), a Pew International Foundation Fellowship (E.W.), and an Institutional National Research Service Award (ES07106).

17 November 1997; accepted 11 March 1998

Modular Organization of Cognitive Systems Masked by Interhemispheric Integration

Kathleen Baynes,* James C. Eliassen, Helmi L. Lutsep, Michael S. Gazzaniga

After resection of the corpus callosum, V.J., a left-handed woman with left-hemisphere dominance for spoken language, demonstrated a dissociation between spoken and written language. In the key experiment, words flashed to V.J.'s dominant left hemisphere were easily spoken out loud, but could not be written. However, when the words were flashed to her right hemisphere, she could not speak them out loud, but could write them with her left hand. This marked dissociation supports the view that spoken and written language output can be controlled by independent hemispheres, even though before her hemispheric disconnection, they appeared as inseparable cognitive entities.

One of the central challenges to cognitive neuroscience is to unmask the apparent unitary nature of perceptual, memorial, and cognitive systems. Neuropsychological analyses, functional brain imaging methodologies, and analyses of normal reaction times have contributed to revealing how seemingly unitary processes are made up of multiple components. Frequently these multiple components are distributed across the hemispheres but appear unified because of the integration that is possible through the corpus callosum. Examination of split-brain patients both before and after their surgery is another tool for the unmasking of such processes. Here we use this method to reveal a dissociation between the neural representations involved in spoken and written language. These results are consistent with the view that the brain processes enabling written language do not call upon brain representations responsible for phonological capacity.

V.J., a 44-year-old female with a high school education, has a normal developmental and educational history. Her mother, her only sister, and her only daughter are left-handed. No other member of her immediate family has a seizure disorder. Her first seizure occurred when she was 16-and-a-half. V.J. is deaf in her right ear as a result of injuries incurred during a seizure episode in her early 30's. She elected to undergo surgery to resect the corpus callosum after

K. Baynes, Center for Neuroscience, University of California at Davis, Davis, CA 95616, and VA Northern California Health Care System, Martinez, CA 94553, USA.
J. C. Eliassen, Center for Neuroscience, University of California at Davis, Davis, CA 95616, USA.
H. L. Lutsep, Oregon Stroke Center, Oregon Health Sciences University, Portland, OR 97201, USA.
M. S. Gazzaniga, Center for Cognitive Neuroscience, Dartmouth College, Hanover, NH 03654, USA.

*To whom correspondence should be addressed at Center for Neuroscience, University of California at Davis, Davis, CA 95616, USA. E-mail: kbaynes@ucdavis.edu